Published in final edited form as:
Pharm Res. 2014 March ; 31(3): 554–565. doi:10.1007/s11095-013-1180-7.

Near-infrared light sensitive liposomes for the enhanced photothermal tumor treatment by the combination with chemotherapy

Jian You[1,*], **Peizun Zhang**[1], **Fuqiang Hu**[1], **Yongzhong Du**[1], **Hong Yuan**[1], **Jiang Zhu**[2,*], **Zuhua Wang**[1], **Jialin Zhou**[1], and **Chun Li**[2]

[1]College of Pharmaceutical Sciences, Zhejiang University, Yuhangtang Road 866, Hangzhou 310058, People's Republic of China

[2]Sir Run Run Shaw Hospital, Zhejiang University School of Medicine, East Qingchun Road 3, Hangzhou 310016, People's Republic of China

[3]Department of Experimental Diagnostic Imaging, The University of Texas MD Anderson Cancer Center, Houston, Texas 77030, USA

Abstract

Purpose—To develop a near-infrared (NIR) light-sensitive liposome, which contains hollow gold nanospheres (HAuNS) and doxorubicin (DOX), and evaluate their potential utility for enhancing antitumor activity and controlling drug release.

Methods—The liposomes (DOX&HAuNS-TSL) were designed based on a thermal sensitive liposome (TSL) formulation, and hydrophobically modified HAuNS were attached onto the membrane of the liposomes. The behavior of DOX release from the liposomes was investigated by the dialysis, diffusion in agarose gel and cellular uptake of the drug. The biodistribution of DOX&HAuNS-TSL was assessed by i.v. injection in tumor-bearing nude mice. Antitumor efficacy was evaluated both histologically using excised tissue and intuitively by measuring the tumor size and weight.

Results—Rapid and repetitive DOX release from the liposomes (DOX&HAuNS-TSL), could be readily achieved upon NIR laser irradiation. The treatment of tumor cells with DOX&HAuNS-TSL followed by NIR laser irradiation showed significantly greater cytotoxicity than the treatment with DOX&HAuNS-TSL alone, DOX-TSL alone (chemotherapy alone) and HAuNS-TSL plus NIR laser irradiation (Photothermal ablation, PTA, alone). In vivo antitumor study indicated that the combination of simultaneous photothermal and chemotherapeutic effect mediated by DOX&HAuNS-TSL plus NIR laser presented a significantly higher antitumor efficacy than the PTA alone mediated by HAuNS-TSL plus NIR laser irradiation.

[*]**Corresponding Author**: Jian You, College of Pharmaceutical Sciences, Zhejiang University, Yuhangtang Road 866, Hangzhou 310058, People's Republic of China; Tel: 086-571-88208443; Fax: 086-571-88208439; youjiandoc@zju.edu.cn. Jiang Zhu, Sir Run Run Shaw Hospital, Zhejiang University School of Medicine, East Qingchun Road 3, Hangzhou 310016, People's Republic of China; zhujiang1963@126.com..

Disclosure of Potential Conflicts of Interest
No potential conflicts of interest were disclosed.

Conclusions—Our study could be as the valuable reference and direction for the clinical application of PTA in tumor therapy.

Keywords

Light sensitive liposomes; Photothermal effect; Controlled release

Introduction

Photothermal ablation (PTA) uses heat generated through absorption of near-infrared light (NIR) to directly destroy tissue. So far, several kinds of gold nanoparticles, such as gold-silica nanoshells (1, 2), gold nanorods (3), gold nanocages (4) and gold colloidal nanospheres (5), have been used as photothermal conducting agent to ablate tumors. To treat a tumor, gold nanoparticles are systemically administered to the subject and allowed to localize to the tumor. The tumor is then exposed to an excitation source, NIR laser light. The gold nanoparticles absorb the incident energy and convert it into heat, which raises the temperature of the tissue and ablates the cancerous cells. Unlike other thermal conducting methods, such as radiofrequency (6), microwave (7), and focused ultrasound ablation therapies (8), gold nanoparticles-mediated-PTA induces a specific heating delivery to targets and presents a promising application for tumor treatment (9). The most extensively developed of these potential applications, gold-silica nanoshells mediated PTA, is currently being studied in early clinical trials (10). However, complete tumor eradication by PTA alone is difficult because the distribution of gold nanoparticles in tumors is often uneven, which induces the heterogeneous heat distribution and sublethal thermal dose in some areas of the tumor.

Liposomes currently represent one of the best studied types of drug carriers and are being used clinically either for experimental drug in various stages of clinical trials or for an approved and established drug. However, their application and development were vastly limited by the slow release of the encapsulated drug, and controlling the encapsulated drug release from liposomes both spatially and temporally still remained a challenge (11-13). Different methods have been applied to solve the problem, such as pH (14, 15), light (16, 17), enzymatic activity (18, 19), ultrasound (20), and temperature (21). As we know, only a few studies have explored the triggered release of liposomes based on a photothermal effect mediated by NIR light and further involved in the application in vivo. For example, Abhiruchi A. group and Ji-Ho Park group employed the similar strategy, which is to mix Doxorubicin (DOX) loaded liposomes with free Gold Nanorods to obtain a triggered release of DOX from liposomes under NIR light irradiation (22, 23). Marek Romanowski group revealed a method for NIR light-induced content release from gold-coated liposomes (24, 25).

Hollow gold nanospheres (HAuNS) are a novel class of gold nanoparticles that have plasmon absorption in the near-infrared (NIR) region and that display a strong photothermal conducting property. HAuNS' unique combination of small size (30–50 nm in diameter) and strong and tunable (520–950 nm) absorption band suggests that HAuNS are a promising photothermal conducting agent for a variety of biomedical applications, including imaging

(26, 27) and cancer therapy (28). Our previous studies have explored the potential utility of HAuNS as a novel delivery vehicle to shuttle biomolecules or to trigger drug release under NIR light irradiation (29-31).

Here, we provided a novel NIR light sensitive liposome containing DOX and HAuNS (DOX&HAuNS-TSL). The liposomes were designed based on a thermal sensitive liposome (TSL) formulation, and HAuNS were attached onto the membrane of the liposomes (Fig. 1A). We hypothesized that, due to the attachment of HAuNS, the liposomes can present the photothermal effect, and consequently a controlled release of the drug by a NIR laser light irradiation as the external stimulus. We also hypothesized the antitumor activity in vivo of DOX&HAuNS-TSL can be significantly enhanced under the NIR laser irradiation by the combination of PTA and chemotherapy, compared with that of HAuNS-TSL , which presented the alone efficacy of PTA.

Materials and Methods

Materials

Sodium citrate (>99%), cobalt chloride hexahydrate (99.99%), sodium borohydride (99%), and chloroauric acid trihydrate (American Chemical Society reagent grade) were purchased from Thermo Fisher Scientific (Waltham, MA) and were used as received. Octadecyl-3-Mercaptopionate (OMP) was from Chemical Indoustry Co.(Japan). Doxorubicin.HCl (DOX) was gifted from Zhejiang Hisun Pharmaceutical Co, Ltd, (Taizhou Zhejiang, China). 1,2-dipalmitoyl-sn-glycero-3-phosphatidylcholine (DPPC), Egg phosphatidylcholine (EPC), Dipalmitoylphosphatidylcholine (DPPC), Hydrogenated soybean phosphatidylcholine (HSPC), cholesterol (Chol), and 1,2-distearoyl-sn-glycero-3-phosphoethanolamine-N-[methoxy(polyethyleneglycol)-2000] (DSPE-PEG_{2000}) were purchased from Lipoid (Germany). 1,1’-dioctadecyl-3,3,3,3’-tetramethylindodicarbocyanine, 4-chlorobenzenesulfonate salt (DiD), 1,1'-Dioctadecyl-3,3,3',3'-Tetramethylindotricarbocyanine Iodide (DiR) were obtained from Invitrogen (Carlsbad, CA, USA). 3-(4,5-dimethylthiazol-2-yl)-2,5 -diphenyltetrazolium bromide (MTT) were purchased from Sigma (St Louis, MO). All other solvents were of analytical or chromatographic grade.

Cell culture

BEL-7402 (human liver carcinoma) cells were obtained from Institute of Biochemistry and Cell Biology (Shanghai, China). The cells were maintained in Dulbecco's modified Eagle's medium containing 10% fetal bovine serum (Life Technologies, Inc., Carlsbad, CA) at 37°C in a humidified atmosphere containing 5% CO_2.

The synthesis and hydrophobic modification of HAuNS

Hollow gold nanospheres (HAuNS) were synthesized according to our published approaches (29). Briefly, 1 mL of cobalt chloride (0.4 M) was mixed with 4.5 mL of sodium borohydride (1 M) and 2.8 mL of sodium citrate (0.1 M). Cobalt chloride was reduced by sodium borohydride to obtain cobalt nanoparticles. Then, chloroauric acid was added into the solution containing cobalt nanoparticles, and the cobalt immediately reduced the gold

ions onto the surface of the nanoparticles and was simultaneously oxidized to cobalt oxide. HAuNS was obtained after the oxidation of remaining cobalt by air. HAuNS was further modified hydrophobically by Octadecyl-3-Mercaptopionate (OMP). First, 0.2 mL of HAuNS [200 optical density (OD), 10.0 mg/mL] were centrifuged at 10,000 rpm for 10min, and the resulting pellets were re-dispersed in 0.5 mL of N,N-Dimethylformamide (DMF). OMP (0.1 mmol) was added to DMF solution containing HAuNS. The reaction was performed overnight at room temperature. OMP modified HAuNS (OMP-HAuNS) was purified by the centrifugation (8000 rpm for 10 min), followed by washing twice with DMF, and then was identified by FT-IR analysis. The size of HAuNS and OMP-HAuNS was determined using dynamic light scattering on a Zetasizer (3000 HS; Malvern Instruments, UK). The UV-visible spectra were recorded on a Beckman Coulter DU-800 UV-visible spectrometer.

Preparation of DOX&HAuNS-TSL

Firstly, HAuNS attached thermal sensitive liposomes (HAuNS-TSL) was prepared by a thin film method. Briefly, OMP-HAuNS (2.5×10^{12} particles) was dispersed in dichloromethane (DCM). DPPC, HSPC, Chol and DSPE-PEG_{2000} (molar ratio of 100:50:15:6, as the total lipid, 50mg) were dissolved in chloroform, and then were mixed with DCM containing OMP-HAuNS. The organic solvents were removed to form a thin lipid film, which was further dried overnight. Then, the lipid film was hydrated at 55 °C for 1h with a 250mM ammonium sulfate buffer. The hydrated lipid vesicles were further sonicated at 55 °C (USC-302, Shanghai Electronic equipment Co., Ltd) to obtain HAuNS-TSL (without DOX loading). The free ammonium sulfate was removed by dialysis for 72 h at room temperature. Secondly, DOX loading into HAuNS-TSL were performed according to the active loading method using an ammonium sulfate gradient (32). DOX solution (2 mg/mL) was added to HAuNS-TSL at a weight ratio 1:20 (DOX: the total lipid), and the mixture solution was incubated for 30 min at 50 °C. The obtained DOX&HAuNS-TSL was purified by size-exclusion chromatography using a Sephadex G-50 column eluted with the buffer (10 mM Na_2HPO_4, 2 mM KH_2PO_4, 136.8 mM NaCl, pH 7.4). DOX-TSL (without HAuNS loading) was also prepared according above same methods. The size and zeta potential of various liposomes were measured by dynamic light scattering (DLS) with particle size and zeta analyzers, respectively. The encapsulation efficiency (EE) of DOX within the liposomes was calculated according to the formula Fi/Ft ×100%, where Fi is the amount of DOX loaded in the liposomes and Ft is the initially feeding amount of DOX. The efficiency of HAuNS encapsulation was calculated by using spectrophotometer (λ=800 nm). Briefly, the obtained DOX/HAuNS-TSL was purified by size-exclusion chromatography using a Sephadex G-50 column eluted with PBS. The efficiency of HAuNS attached to liposomes was calculated by comparing the absorption value of initial and purified DOX/HAuNSTSL at the wavelength of 800nm.

Differential scanning calorimetry measurements (DSC)

In order to determine the phase transition temperatures of the liposomes, 50 μL of the sample (blankTSL or DOX&HAuNS-TSL suspensions) were placed in T zero hermetic aluminum pans sealed with lids. The sample were then thermally scanned from 30 to 70 °C

at 10 °C/min heating rate using differential scanning calorimetry (Q200 differential scanning calorimeter, TA Instruments, USA).

NIR-light-triggered release of drug from DOX&HAuNS-TSL

DOX&HAuNS-TSL or DOX-TSL (10 mg) in 1mL PBS (pH 7.4) was transferred into a dialysis membrane bag (MWCO 7 kDa), and then submerged into 10 mL PBS (pH 7.4) under the stirring (100 rpm) at 37 °C. For NIR laser irradiation, the sample was taken out from the dialysis bag at the designed time point, and put into a transparent glass tube. The samples were irradiated with the 808-nm NIR light at an output power of 3 or 6W over a period of 5min (Diomed 15 plus, Cambridge, UK), as our previous reported (30). Then, the sample was put back into the dialysis bag to continue the release study. The release of DOX under no NIR laser irradiation was as control. The released DOX was quantified by fluorescence spectrophotometry (Ex: 505 nm, Em: 565 nm) (F-2500, HITACHI Co., Japan).

NIR-light-triggered release was further investigated by an *in vivo* imaging system (CRI Inc., Woburn, MA). Firstly, DiR, a near-infrared lipophilic fluorescent tracer, was used to label the membrane of the liposomes. Briefly, DiR (0.1 mg) was co-dissolved with the total lipid (50 mg) in chloroform. The liposomes containing DiR were prepared according to the above method in section 2.4, and were purified by going through a Sephadex G-50 column. It was found almost 100% DiR was loaded into the liposomes due to its lipophilic property. Secondly, the agarose gel lump was prepared using the reported methods (33). Briefly, 1g of agarose was brought to boiling in 100 mL AET (0.05 M Tris, 0.02 M sodium acetate, pH 7.4). Then, the solution was added to fill the Petri dish and cooled to room temperature to obtain the agarose gel lump. A circular hole (1 cm diameter and 0.5 cm depth) in the center of agarose gel lump was made to hold the sample. The sample was irradiated by NIR laser (output power of 3 W for 20 min), and then the gel lump was observed by the in vivo imaging system. The fluorescence images of samples were taken before and after NIR laser irradiation, using Maestro 2.10.0 software (CRI Inc., Woburn, MA). Fluorescence images for DOX were acquired using a blue filter set (Ex: 455nm; Em: 560 nm) and an exposure time of 235 ms. Fluorescence images for DiR marked liposomes were acquired using a NIR filter set (Ex: 704nm; Em: 740 nm) and an exposure time of 350 ms. NIR-light-triggered release of DOX from DOX&HAuNS-TSL or DOX-TSL was identified by the diffused degree of DOX molecule in agarose gel.

Furthermore, we investigated NIR-light-triggered release of DOX in tumor cells. Here, we chose DiD to label the membrane of the liposomes instead of DiR for the observation by the confocal microscope. DiD is also a near-infrared lipophilic fluorescent tracer, but has blue-shifted fluorescence excitation and emission spectra, fitting for confocal microscope system, compared with DiR. DiD labeled DOX&HAuNS-TSL and DOX-TSL were prepared according to the same protocol with DiR labeled liposomes. BEL-7402 cells were plated on 10 mm^2 glass coverslips in 24-well culture plates at a density of 5×10^4 cells per well and allowed to attach for 24h, and then were incubated with DiD labeled DOX&HAuNS-TSL or DOX-TSL. After 2h incubation, the medium was refreshed and cells were irradiated with NIR laser at an output of 3w for 5 min. After the another incubation for 2h, the cell monolayer on the coverslips was removed, repeatedly rinsed with PBS, fixed with 4 %

paraformaldehyde and then mounted for confocal microscopic examination (BX61W1-FV1000, Olympus, Japan). Fluorescent imaging of DOX and DiD was obtained by the excitation at 485 nm and 644 nm and the emission at 595 nm and 667 nm, respectively. As controls, cells were incubated with DiD labeled DOX&HAuNSTSL or DOX-TSL under no NIR irradiation.

In vitro cytotoxicity assay

BEL-7402 cells were seeded at a density of 1.0×10^4 per well in 96-well plates and incubated for 24 h to attach. Cells were incubated with various liposomes, and irradiated by NIR laser once (output power of 3 W, 2 min) at the beginning of incubation. Cells under no NIR laser irradiation were as controls. After 72 h incubation, 20 mL MTT (5 mg/mL) was added, and the plates were incubated for an additional 4 h. Culture medium was removed, the formazan crystals were dissolved in 100 mL DMSO, and the absorbance value were read on a microplate reader (Bio-Rad, Model 680, Hercules, CA) at the dual wavelengths of 570 nm. The data are expressed as percentage of survival cells and are reported as the means of triplicate measurements.

In vivo biodistribution studies

All animal studies were carried out under Institutional Animal Care and Use Committee-approved protocols. Male nude mice (18-22 g; 6-8 weeks of age) were inoculated subcutaneously with BEL-7402 cells (5×10^6 cells in 0.1 mL PBS). When the tumor volume reached about $500mm^3$, the mice were injected intravenously with DiR labeled DOX&HAuNS-TSL (0.2 mL/mouse, 20 μg/mL DiR). The mice were observed by the in vivo imaging system at the predetermined time after the injection. At the end of the experiment, the mice were killed. Various tissues, including tumors, were collected, weighted and observed by the in vivo imaging system. The fluorescent intensity, responding the amount of DOX&HAuNS-TSL, was also read by the imaging system. The accumulation of DOX&HAuNS-TSL in various tissues was calculated as %ID/g (the percentage of the injected dose per gram of tissue).

In vivo antitumor activity

BEL-7402 tumors were generated by subcutaneous injection of BEL-7402 cells (5×10^6 cells/mouse). When the mean tumor volume reached approximately 150 mm^3, the mice were randomly allocated into four groups. The mice in group 1 to 4 were injected intravenously for each time with saline (n=6), DOX-TSL (n=6, 4 mg/kg of DOX), HAuNS-TSL (n=6, 2.5×10^{12} particles/Kg of HAuNS), DOX&HAuNS-TSL (n=6, 4 mg/kg of DOX and 2.5×10^{12} particles/Kg of HAuNS), respectively. All mice were injected for total three times on day 1, 3 and 5 (one injection for one day), and all tumors in mice, except for the group of DOX-TSL, were irradiated by NIR laser (2.0 W/cm^2 for 5 minutes) for total three times on day 2, 4 and 6 (one irradiation for one day). Tumor growth was determined every two days by measuring two orthogonal tumor diameters. Tumor volume was calculated according to the formula $(a\times b^2)/2$, where a and b are the long and short diameters of a tumor, respectively. Experiment was terminated on day 22 after initial treatment or when tumors in the control group reached >1000 mm^3.

Statistical analysis was conducted by ANOVA, with $P < 0.05$ considered to be statistically significant.

Results

Preparation of DOX&HAuNS-TSL

In order to increase the encapsulation efficiency of HAuNS into liposomes, we modified hydrophobically the surface of HAuNS by OMP, using the reaction between hydrosulfide group (-SH) in OMP with Au. IR spectrum confirmed the conjugation of OMP on HAuNS (fig. S1): The weak characteristic peak of hydrosulfide group at the range of $2500cm^{-1}$~$2900cm^{-1}$ was disappeared completely for OMP-HAuNS, comparing with OMP alone, which suggested that the group of -SH in OMP changed to-S-Au. HAuNS was negatively charged (−49.6 mv). After the modification of OMP, the zeta potential of OMP-HAuNS was almost neutral (fig. S2). A very narrow size distribution of HAuNS and OMP-HAuNS was presented in fig. S3. The absorption spectra showed that the plasma resonance peaks for OMP-HAuNS were in the NIR region (~800 nm) (Fig. 1B). Thus, OMP modification did not affect the spectrum characteristic of HAuNS.

DSC peak maximums and the phase transition temperature (Tm) of blank TSL and DOX&HAuNS-TSL were at 45.5 and 44.6 °C, and at 42.2 and 40.3 °C, respectively (Fig. 1C). At Tm, gel-crystalline phase of phospholipid bilayers transforms to liquid-crystalline phase, inducing the changes of membrane permeability of the liposomes, which results in the increased release of entrapped drug from the liposomes. Clearly, the loading of DOX and HAuNS did not affect the thermosensitive property of the liposomes. Table S1 and fig. S4 summarized physical properties of DOX-TSL and DOX&HAuNS-TSL. The average diameter of blank TSL was 102.7 nm, determined by DLS. Due to the encapsulation of DOX and HAuNS, the average diameter of DOX&HAuNS-TSL increased significantly to 154.8 nm, determined by DLS. The liposomes presented to be white spheres due to the staining by phosphotungstic acid before the observation by TEM (Fig. 1D). OMP-HAuNS, because of the hydrophobic modification, was mainly attached on the surface (e.g. membrane) of the liposomes. The encapsulation efficiency of DOX for both DOX-TSL and DOX&HAuNS-TSL was over 90%, and almost all of feeding HAuNS after the hydrophobic modification was encapsulated into the liposomes.

NIR-light-triggered release

Continuous exposure of aqueous solution containing DOX&HAuNS-TSL (an HAuNS concentration of 5.0×10^{10} nanoparticles /mL) to NIR light (output power of 3 W) resulted in the rapid elevation of its temperature (from 26.1 °C to 49.9 °C in 5 min). In comparison, no significant temperature change was observed when phosphate-buffered saline (PBS) was exposed to the laser light (fig. S5).

The characteristics of DOX release from DOX-TSL and DOX&HAuNS-TSL is showed in Figure 2A. The solutions containing DOX&HAuNS-TSL were irradiated repeatedly using a NIR laser over a period of 5 min, followed by 4-h intervals with the laser turned off. After a NIR irradiation, a rapid increase in DOX release from DOX&HAuNS-TSL was obtained

during the following 4 h period, when the released DOX diffused through the dialysis membrane into the external medium. For twice NIR irradiations at the output power of 3W, the increased release of DOX in 4h after each irradiation was about 4.1% and 7.4% for first and second NIR irradiation respectively, which finally induced the total release of about 20% DOX after 24 h. Significantly more DOX will be released from DOX&HAuNS-TSL when the output power of NIR irradiation was increased. Under the irradiation of the output power of 6W, the increased release of DOX in 4h after each irradiation was about 16.0 % and 16.1 % for first and second NIR irradiation respectively, which finally induced the total accumulative release of about 40% DOX after 24 h. However, almost no DOX release from DOX&HAuNS-TSL under no NIR irradiation, except for a little burst release of DOX during the initial 2h, inducing the release of 3.4% DOX. Only 2.1% DOX was further released from DOX&HAuNS-TSL from 2 to 24h due to no NIR laser irradiation. Because there was no HAuNS in DOX-TSL, characteristics of DOX release from DOX-TSL (with or without NIR laser irradiation) were similar with that of DOX&HAuNS-TSL under no NIR irradiation.

Because only free DOX molecules, but not entrapped in the liposomes, can diffuse in the agarose gel, we can investigate the triggered-release of DOX from DOX&HAuNSTSL by the imaging system (Fig. 2B). DiR can combine hard with lipid component in the membrane of the liposomes due to its highly lipophilic property, which can be used to mark DOX&HAuNS-TSL. The yellow circle indicated the location of the hole, where the sample was placed. For DOX&HAuNS-TSL, many DOX molecules (red fluorescence) diffused out the hole under a NIR laser irradiation, while the liposomes (green fluorescence) still stayed in the hole. As control, almost no DOX molecule diffused into the gel under the laser irradiation for DOX-TSL (no HAuNS), like that for DOX&HAuNSTSL or for DOX-TSL under no laser irradiation. These results obviously indicated HAuNS in the liposomes produced the photothermal effect under NIR laser irradiation, which consequently triggered the release of DOX from DOX&HAuNS-TSL.

After the internalization of DOX&HAuNS-TSL or DOX-TSL, only DOX released from the liposomes can enter into cell nuclei, while DOX entrapped in the liposomes will stay in cytoplasm (Fig. 2C). After total 4 h incubation, the strong red and green fluorescence signal were observed, and limited to spots scattered throughout the cytoplasm but not in nuclei, which indicated that both DOX&HAuNS-TSL and DOX-TSL were internalized into BEL-7402 cells and were retained in the endolysosomal compartments. Furthermore, the green fluorescence signal from DiD indicated the presence of the liposomes, which to a large extent colocalized with DOX. These results indicated that almost no DOX was released from DOX&HAuNS-TSL or DOX-TSL during this time. However, for DOX&HAuNS-TSL, under a NIR laser irradiation, some red fluorescence signal was observed in cell nuclei, while green fluorescence signal still stay in cytoplasm, which indicated some DOX was released from DOX&HAuNS-TSL and distributed into cell nuclei due to NIR-light-triggered release. Because some DOX was released from DOX&HAuNS-TSL, red fluorescence signal became weaker compared with green fluorescence signal. For DOX-TSL, almost no DOX was released under NIR irradiation, like that under no NIR irradiation, because there was no HAuNS in the liposomes (Fig. 2C).

In vitro cytotoxicity assay—Figure 3 shows the cytotoxic effects of free DOX, DOXTSL, HAuNS-TSL and DOX&HAuNS-TSL, with or without NIR laser irradiation, in BEL-7402 cells. The cell-killing efficiency of DOX&HAuNS-TSL combined with NIR laser irradiation, similar to free DOX, was significantly higher than that of DOX&HAuNS-TSL or DOX-TSL alone. For example, almost 90% tumor cells were killed after 72h incubation with DOX&HAuNS-TSL combining the irradiation at the concentration of 1μM. However, about 60% and 70% cells were survived for DOX&HAuNS-TSL and, respectively, under the same condition but no NIR irradiation (Fig. 3A). NIR laser irradiation did not induce the significant increase on cytotoxicity of DOX-TSL because of no HAuNS in the liposomes (Fig. 3B). Clearly, the significantly enhanced cytotoxicity of DOX&HAuNS-TSL combined with NIR laser irradiation was much higher than that of photothermal ablation alone (HAuNS-TSL plus NIR) (Fig. 3C) or DOX cytotoxicity alone (DOX-TSL plus NIR laser) (Fig. 3D). For example, under NIR irradiation, only 12% and 30% cells were killed for DOX-TSL and HAuNS-TSL after 72 h incubation (1 μM), respectively, but 90% cells was killed for DOX&HAuNS-TSL under the same condition. These results indicated that enhanced cytotoxicity of DOX&HAuNS-TSL plus NIR irradiation should be attributed to the combination and synergistic interaction of photothermal ablation of HAuNS and cytotoxic activity of released DOX, like our previously reported (30).

***In vivo* biodistribution studies—**The *in vivo* imaging of DiR marked DOX&HAuNSTSL was shown in Figure 4. It was clear that there was an increased accumulation of DOX&HAuNS-TSL in BEL-7402 tumors from 1 to 24 h, and subsequently the accumulative amount of the liposomes in the tumors decreased gradually (Fig. 4A). The accumulation of DOX&HAuNS-TSL in the tumors should be attributed to the enhanced permeability and retention effect of the liposomes. The fluorescent intensity of various tissues after 6, 24 and 48h injection was observed (Fig. 4B), and was quantitated. There was the highest accumulation of DOX&HAuNS-TSL at 24h (10.9% ID) after injection in the tumors, compared with 6h (4.2% ID) and 48h (7.4% ID) (Fig. 4C). Because the fluorescent probe (DiR) was used to label the membrane of liposomes, the obtained fluorescent signal actually presented an in vivo distribution of the liposomes.

***In vivo* antitumor activity—**Figure 5A shows the BEL-7402 tumor growth curves after intravenous injections (three times) of saline, DOX-TSL (total 12 mg/kg of DOX), HAuNS-TSL (total 7.5×10^{12} particles/Kg of HAuNS), DOX&HAuNS-TSL (total 12 mg/kg of DOX and 7.5×10^{12} particles/Kg of HAuNS). Mice in each group, except for DOX-TSL group, received NIR laser treatment (2.0 W/cm^2 for 5 min) 24 h after each injection. The mice in the saline-plus-laser group were killed on day 12 after injection because most of the tumors in this group were ~1000 mm^3 at that time. Mice in the other three groups were killed on day 22. Treatment with DOX&HAuNS-TSL-plus-laser showed significantly higher antitumor activity compared with saline-plus-laser, HAuNS-TSL-plus-laser, and DOX-TSL (Fig. 5B). The mean tumor weight in DOX&HAuNS-TSL-plus-laser group on day 22 after treatment was 4.7 ± 5.2 mg (n = 6), which was significantly smaller than that of the saline-plus-laser (931.5 ± 295.4 mg on day 12, n = 6; $P<0.0001$), HAuNS-TSL-plus-laser (83.8 ± 80.1 mg, n=6; $P<0.001$), and DOX-TSL (358.2 ± 95.2 mg, n = 6; $P<0.0001$) groups (Fig. 5C). In DOX&HAuNS-TSL-plus-laser group, the tumors in 2 of the six mice treated

disappeared completely and became small scar tissue by 22 days after the injection (Fig. 5D). Histological analysis showed the presence of scar tissue and a lack of residual tumor cells in mice treated with DOX&HAuNS-TSL-plus-laser (Fig. 6A, left). The tumors in other 4 mice in this group became very small, and Histological analysis showed that the structure of these tumors was destroyed seriously (Fig. 6A, right). However, in HAuNS-TSL-plus-laser group, though the original tumors in 3 of six mice looked disappeared and became scar tissue, the new tumors appeared near the scar tissue (Fig. 5D), and histological analysis showed the tumors had a full structure and suggested that these tumors were not fully resolved (Fig. 6B, left). Furthermore, histological analysis of the scar tissue discovered the survival tumor tissue (Fig. 6B, right), with an intact structure like that of the tumors in saline group (Fig. 6C), which suggested still high activity of these tumors.

Discussion

Though it was reported by Joseph A. Zasadzinski et al that liposomes containing hollow gold nanoshells were employed to control release of the entrapped agent, a fluorescent dye, under a NIR light irradiation, there was no further work focusing on therapeutic study in vitro and in vivo (34). Furthermore, the size of the reported liposomes containing hollow gold nanoshells was about 0.5~1 μm, which obviously was not fit for the administration of *iv* injection. Here, we synthesized HAuNS using a template of cobalt nanoparticles, instead of silver nanoparticles, which was employed as the template for the synthesis of Hollow gold nanoshells. As a result, HAuNS presented a narrow size distribution and strong photothermal converting efficiency. Our TSL containing HAuNS had a smaller diameter (<200nm), which was fit for systemic administration for therapeutic application. In our previous study (29), DOX, due to the positive charge, was absorbed directly onto the surface of HAuNS via electrostatic interaction. Herein, for DOX/HAuNS-TSL, the liposomes can load both hydrophilic and hydrophobic drugs, which is independent of the potential of drugs. So, DOX/HAuNS-TSL may present a wider application than that of HAuNS alone.

In this study, we showed that significantly increased DOX release from DOX&HAuNS-TSL under NIR laser irradiation, while almost no DOX was released from the liposomes under the same condition but no NIR laser irradiation. The triggered-release of DOX should be attributed to the photothermal effect produced by HAuNS in TSL. The possible mechanisms are: 1) The photothermal effect induces the perturbation and increased permeability of local liposome membrane near HAuNS during the NIR irradiation period; 2) The heat, generated by HAuNS under NIR irradiation, elevates temperature of whole liposomes due to its diffusion and longer duration, results in the permeability increase of whole liposome membrane due to the phase transformation of phospholipid bilayers, and consequently triggers the release of encapsulated DOX.

In order to investigate which mechanism may play the main role for the triggered release, we prepared the liposomes containing DOX and HAuNS (DOX&HAuNS-NTSL), based on the non-thermal sensitive liposome (NTSL) formulation, by the same methods for DOX&HAuNS-TSL. The total lipid was composed of EPC: Chol: $DSPEPEG_{2000}$=90:10:6 (molar ratio). DSC measurement demonstrated that there was no phase transition temperature for both blank NTSL and DOX&HAuNS-NTSL (fig. S6). The size and DOX

EE of DOX&HAuNS-NTSL, summarized in Table S1, were similar with those of DOX&HAuNS-TSL. Under NIR laser irradiation, only 4.3% DOX was released from DOX&HAuNS-NTSL at 12h (fig. S7), while 16.8% DOX was released from DOX&HAuNS-TSL under the same condition (Fig. 2A). Furthermore, for DOX&HAuNSNTSL, NIR laser irradiation induced a release increase of only 2.5% DOX. These results indicated that the diffusion of heat resulted in the phase transition and the increased permeability of whole liposome membrane should be the main contribution of the triggered release of DOX from DOX&HAuNS-TSL.

Figure 4B obviously showed that the fluorescence signal was uneven in the tumor.

The weak signal in some areas of the tumor indicated that the lack of DOX&HAuNS-TSL in the areas. As a result, the only thermal dose, generated by HAuNS under the NIR laser irradiation, will be not sufficient for killing all of cancer cells in the areas of the tumor if there is no toxicity efficacy of DOX, which may induce the tumor recurrence after the treatment. The significantly enhanced cytotoxicity for DOX&HAuNS-TSL versus HAuNS-TSL alone (PTA alone) under NIR laser irradiation was obtained, and should be attributed three effects: 1) the PTA effect, 2) increased intracellular DOX concentration due to the triggered release of DOX from DOX&HAuNS-TSL, which was demonstrated in Figure 2C, and 3) a synergistic interaction between the photothermal effect and DOX's cytotoxic effect. The synergistic cytotoxic effects between chemotherapeutic agent and hyperthermia have been well documented in previous other work (35-38). Our finding of in vivo antitumor study further demonstrated that DOX&HAuNS-TSL, with the combination of photothermal and chemotherapeutic effect under NIR laser irradiation, presented significantly higher antitumor efficacy than HAuNS-TSL-plus-NIR laser (PTA alone) and DOX-TSL (chemotherapeutic effect alone) (Fig. 5 and 6). Our next work will focus on the detail mechanism investigation of the synergistic therapy by DOX&HAuNSTSL-plus NIR laser.

Conclusion

We provided a novel NIR light sensitive liposome, which contains HAuNS and DOX, and presents photothermal effect and controlled release of DOX by NIR laser light irradiation. Rapid and repetitive DOX release from the liposomes (DOX&HAuNS-TSL) could be readily achieved upon NIR laser irradiation, which could be mainly attributed to the phase transition and the increased permeability of whole liposome membrane due to the heat diffusion from HAuNS attached on the membrane. Our data also indicated the treatment of tumor cells with DOX&HAuNS-TSL followed by NIR laser irradiation showed significantly greater cytotoxicity than the treatment with DOX&HAuNS-TSL alone, DOX- TSL alone (chemotherapy alone) and HAuNS-TSL plus NIR laser irradiation (PTA alone). The significantly enhanced cytotoxicity for DOX&HAuNS-TSL plus NIR laser should be attributed three effects: 1) the PTA effect, 2) increased intracellular DOX concentration due to the triggered release of DOX from DOX&HAuNS-TSL, and 3) a synergistic interaction between the photothermal effect and DOX's cytotoxic effect. Furthermore, our finding of in vivo antitumor study indicated that the combination of simultaneous photothermal and chemotherapeutic effect mediated by DOX&HAuNS-TSL plus NIR laser presented a significantly higher antitumor efficacy than the PTA alone mediated by HAuNS-TSL plus

NIR laser irradiation. Our study could be as the valuable reference and direction for the clinical application of PTA in tumor therapy.

Supplementary Material

Refer to Web version on PubMed Central for supplementary material.

Acknowledgments

This work was supported by the National Nature Science Foundation of China (81001411), Qianjiang Talent Plan Program of Zhejiang Province (2013R10043), the National Basic Research Program of China (973 Program) under Contract 2009CB930300, National Nature Science Foundation of China (81072583), and part by the National Cancer Institute (U54CA151668).

References

1. Loo C, Lowery A, Halas N, West J, Drezek R. Immunotargeted nanoshells for integrated cancer imaging and therapy. Nano Lett. 2005; 5:709–711. [PubMed: 15826113]
2. Schwartz JA, Shetty AM, Price RE, Stafford RJ, Wang JC, Uthamanthil RK, Pham K, McNichols RJ, Coleman CL, Payne JD. Feasibility study of particle-assisted laser ablation of brain tumors in orthotopic canine model. Cancer Res. 2009; 69:1659–1667. [PubMed: 19208847]
3. von Maltzahn G, Park J-H, Agrawal A, Bandaru NK, Das SK, Sailor MJ, Bhatia SN. Computationally guided photothermal tumor therapy using long-circulating gold nanorod antennas. Cancer Res. 2009; 69:3892–3900. [PubMed: 19366797]
4. Chen J, Glaus C, Laforest R, Zhang Q, Yang M, Gidding M, Welch MJ, Xia Y. Gold nanocages as photothermal transducers for cancer treatment. Small. 2010; 6:811–817. [PubMed: 20225187]
5. Abdulla-Al-Mamun M, Kusumoto Y, Mihata A, Islam MS, Ahmmad B. Plasmon-induced photothermal cell-killing effect of gold colloidal nanoparticles on epithelial carcinoma cells. Photochemical & Photobiological Sciences. 2009; 8:1125–1129. [PubMed: 19639114]
6. Wong SL, Mangu PB, Choti MA, Crocenzi TS, Dodd GD 3rd, Dorfman GS, Eng C, Fong Y, Giusti AF, Lu D, Marsland TA, Michelson R, Poston GJ, Schrag D, Seidenfeld J, Benson AB 3rd. American Society of Clinical Oncology 2009 clinical evidence review on radiofrequency ablation of hepatic metastases from colorectal cancer. J Clin Oncol. 2010; 28:493–508. [PubMed: 19841322]
7. Dooley WC, Vargas HI, Fenn AJ, Tomaselli MB, Harness JK. Focused microwave thermotherapy for preoperative treatment of invasive breast cancer: a review of clinical studies. Ann Surg Oncol. 2010; 17:1076–1093. [PubMed: 20033319]
8. Orsi F, Zhang L, Arnone P, Orgera G, Bonomo G, Vigna PD, Monfardini L, Zhou K, Chen W, Wang Z, Veronesi U. High-intensity focused ultrasound ablation: effective and safe therapy for solid tumors in difficult locations. AJR Am J Roentgenol. 2010; 195:W245–252. [PubMed: 20729423]
9. Kennedy LC, Bickford LR, Lewinski NA, Coughlin AJ, Hu Y, Day ES, West JL, Drezek RA. A New Era for Cancer Treatment: Gold - Nanoparticle - Mediated Thermal Therapies. Small. 2011; 7:169–183. [PubMed: 21213377]
10. [September 2010] Pilot Study of AuroLase Therapy in Refractory and/or Recurrent Tumors of the Head and Neck. 2010. http://clinicaltrials.gov/ct2/show/NCT00848042
11. Peer D, Karp JM, Hong S, Farokhzad OC, Margalit R, Langer R. Nanocarriers as an emerging platform for cancer therapy. Nat Nanotechnol. 2007; 2:751–760. [PubMed: 18654426]
12. Sengupta S, Eavarone D, Capila I, Zhao G, Watson N, Kiziltepe T, Sasisekharan R. Temporal targeting of tumour cells and neovasculature with a nanoscale delivery system. Nature. 2005; 436:568–572. [PubMed: 16049491]
13. Abraham SA, Waterhouse DN, Mayer LD, Cullis PR, Madden TD, Bally MB. The liposomal formulation of doxorubicin. Methods Enzymol. 2005; 391:71–79. [PubMed: 15721375]

14. Obata Y, Tajima S, Takeoka S. Evaluation of pH-responsive liposomes containing amino acid-based zwitterionic lipids for improving intracellular drug delivery in vitro and in vivo. J Control Release. 2010; 142:267–276. [PubMed: 19861141]
15. Ducat E, Deprez J, Gillet A, Noel A, Evrard B, Peulen O, Piel G. Nuclear delivery of a therapeutic peptide by long circulating pH-sensitive liposomes: benefits over classical vesicles. Int J Pharm. 2011; 420:319–332. [PubMed: 21889584]
16. Paasonen L, Laaksonen T, Johans C, Yliperttula M, Kontturi K, Urtti A. Gold nanoparticles enable selective light-induced contents release from liposomes. J Control Release. 2007; 122:86–93. [PubMed: 17628159]
17. Paasonen L, Sipila T, Subrizi A, Laurinmaki P, Butcher SJ, Rappolt M, Yaghmur A, Urtti A, Yliperttula M. Gold-embedded photosensitive liposomes for drug delivery: triggering mechanism and intracellular release. J Control Release. 2010; 147:136–143. [PubMed: 20624434]
18. Stadler B, Chandrawati R, Price AD, Chong SF, Breheney K, Postma A, Connal LA, Zelikin AN, Caruso F. A microreactor with thousands of subcompartments: enzyme-loaded liposomes within polymer capsules. Angew Chem Int Ed Engl. 2009; 48:4359–4362. [PubMed: 19418505]
19. Vamvakaki V, Fournier D, Chaniotakis NA. Fluorescence detection of enzymatic activity within a liposome based nano-biosensor. Biosens Bioelectron. 2005; 21:384–388. [PubMed: 16023967]
20. Dromi S, Frenkel V, Luk A, Traughber B, Angstadt M, Bur M, Poff J, Xie J, Libutti SK, Li KC, Wood BJ. Pulsed-high intensity focused ultrasound and low temperature-sensitive liposomes for enhanced targeted drug delivery and antitumor effect. Clin Cancer Res. 2007; 13:2722–2727. [PubMed: 17473205]
21. Li L, ten Hagen TL, Schipper D, Wijnberg TM, van Rhoon GC, Eggermont AM, Lindner LH, Koning GA. Triggered content release from optimized stealth thermosensitive liposomes using mild hyperthermia. J Control Release. 2010; 143:274–279. [PubMed: 20074595]
22. Agarwal A, Mackey MA, El-Sayed MA, Bellamkonda RV. Remote triggered release of doxorubicin in tumors by synergistic application of thermosensitive liposomes and gold nanorods. ACS Nano. 2011; 5:4919–4926. [PubMed: 21591812]
23. Park JH, von Maltzahn G, Ong LL, Centrone A, Hatton TA, Ruoslahti E, Bhatia SN, Sailor MJ. Cooperative nanoparticles for tumor detection and photothermally triggered drug delivery. Adv Mater. 2010; 22:880–885. [PubMed: 20217810]
24. Leungand M SJ. Romanowski. NIR-activated content release from plasmon resonant liposomes for probing single-cell responses. ACS Nano. 2012; 6:9383–9391. [PubMed: 23106797]
25. Leung SJ, Bobnick MC, Romanowski M. Plasmon resonant gold-coated liposomes for spectrally controlled content release. Proc Soc Photo Opt Instrum Eng. 2010:7577.
26. Schwartzberg AM, Oshiro TY, Zhang JZ, Huser T, Talley CE. Improving nanoprobes using surface-enhanced Raman scattering from 30-nm hollow gold particles. Anal Chem. 2006; 78:4732–4736. [PubMed: 16808490]
27. Lu W, Huang Q, Ku G, Wen X, Zhou M, Guzatov D, Brecht P, Su R, Oraevsky A, Wang LV, Li C. Photoacoustic imaging of living mouse brain vasculature using hollow gold nanospheres. Biomaterials. 2010; 31:2617–2626. [PubMed: 20036000]
28. Lu W, Xiong C, Zhang G, Huang Q, Zhang R, Zhang JZ, Li C. Targeted photothermal ablation of murine melanomas with melanocyte-stimulating hormone analog-conjugated hollow gold nanospheres. Clin Cancer Res. 2009; 15:876–886. [PubMed: 19188158]
29. You J, Zhang G, Li C. Exceptionally high payload of doxorubicin in hollow gold nanospheres for near-infrared light-triggered drug release. ACS Nano. 2010; 4:1033–1041. [PubMed: 20121065]
30. You J, Shao R, Wei X, Gupta S, Li C. Near-infrared light triggers release of Paclitaxel from biodegradable microspheres: photothermal effect and enhanced antitumor activity. Small. 2010; 6:1022–1031. [PubMed: 20394071]
31. You J, Zhang R, Zhang G, Zhong M, Liu Y, Van Pelt CS, Liang D, Wei W, Sood AK, Li C. Photothermal-chemotherapy with doxorubicin-loaded hollow gold nanospheres: A platform for near-infrared light-trigged drug release. J Control Release. 2012; 158:319–328. [PubMed: 22063003]

32. de Smet M, Langereis S, den Bosch S.v. Grüll H. Temperature-sensitive liposomes for doxorubicin delivery under MRI guidance. Journal of Controlled Release. 2010; 143:120–127. [PubMed: 19969035]
33. Noble RP, Hatch FT, Mazrimas JA, Lindgren FT, Jensen LC, Adamson GL. Comparison of lipoprotein analysis by agarose gel and paper electrophoresis with analytical ultracentrifugation. Lipids. 1969; 4:55–59. [PubMed: 5766850]
34. Wu G, Mikhailovsky A, Khant HA, Fu C, Chiu W, Zasadzinski JA. Remotely triggered liposome release by near-infrared light absorption via hollow gold nanoshells. J Am Chem Soc. 2008; 130:8175–8177. [PubMed: 18543914]
35. Hahnand GM, Shiu EC. Effect of pH and elevated temperatures on the cytotoxicity of some chemotherapeutic agents on Chinese hamster cells in vitro. Cancer Res. 1983; 43:5789–5791. [PubMed: 6196107]
36. Yooand J, Lee YJ. Effect of hyperthermia and chemotherapeutic agents on TRAIL-induced cell death in human colon cancer cells. J Cell Biochem. 2008; 103:98–109. [PubMed: 17520700]
37. Adachi S, Kokura S, Okayama T, Ishikawa T, Takagi T, Handa O, Naito Y, Yoshikawa T. Effect of hyperthermia combined with gemcitabine on apoptotic cell death in cultured human pancreatic cancer cell lines. Int J Hyperthermia. 2009; 25:210–219. [PubMed: 19437237]
38. Ko SH, Ueno T, Yoshimoto Y, Yoo JS, Abdel-Wahab OI, Abdel-Wahab Z, Chu E, Pruitt SK, Friedman HS, Dewhirst MW, Tyler DS. Optimizing a novel regional chemotherapeutic agent against melanoma: hyperthermia-induced enhancement of temozolomide cytotoxicity. Clin Cancer Res. 2006; 12:289–297. [PubMed: 16397054]

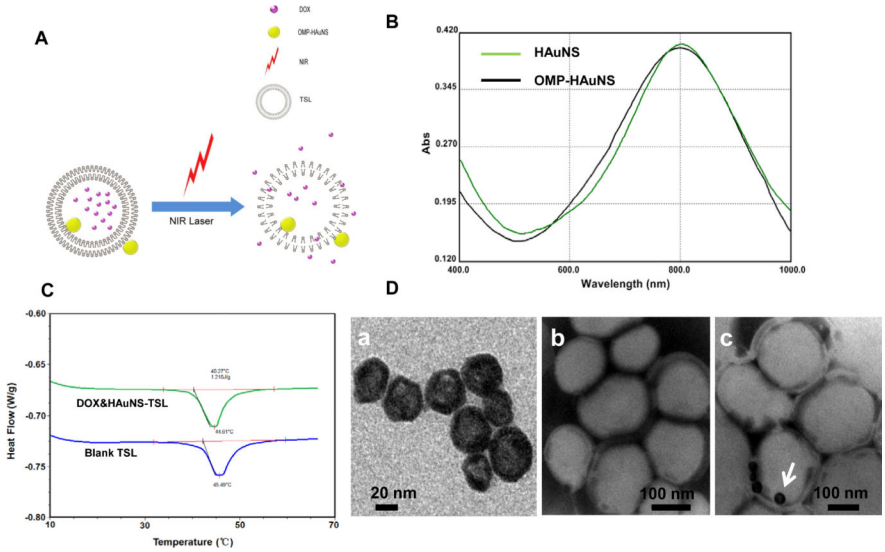

Figure 1.

(A) Hypothetical structure of DOX&HAuNS-TSL and the triggered drug release under NIR laser irradiation. (B) The absorption spectra of HAuNS and OMPHAuNS, which showed that the plasma resonance peaks for both HAuNS and OMP-HAuNS were in the NIR region (~800 nm). (C) DSC peak maximums and the phase transition temperature (Tm) of blank TSL and DOX&HAuNS-TSL. (D) TME image of HAuNS (a), blank TSL (b) and DOX/HAuNS-TSL (c). The samples were stained by phosphotungstic acid before the observation. The liposomes presented to be white spheres, and OMP-HAuNS (the write arrow) was mainly attached on the surface (e.g. membrane) of the liposomes.

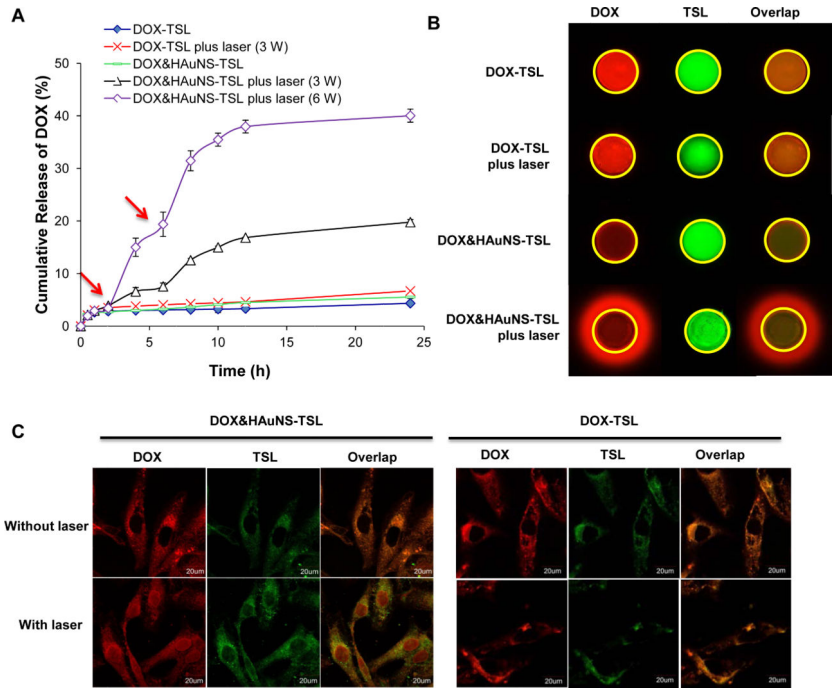

Figure 2.

(A) NIR-light-triggered release of DOX from DOX&HAuNS-TSL by NIR laser over a period of 5 min at the output power of 3W (triangle) or 6W (diamond) and DOX-TSL by NIR laser over a period of 5 min at the output power of 3W (cross). DOX release from DOX-TSL (solid diamond) and DOX&HAuNS-TSL (traverse) without NIR laser irradiation was as controls. Red arrows indicate the beginning time points of NIR laser irradiation. (B) The triggered-release of DOX from DOX&HAuNS-TSL mediated by NIR laser irradiation (3W for 20 min), which was observed by in vivo imaging system. Yellow circle indicated the location of the hole in the agarose gel, where the sample was put. Red fluorescent signal out of the yellow circle represented the released DOX molecule from the micelles. (C) Cell uptake of DOX&HAuNS-TSL and DOX-TSL followed by NIR laser irradiation. The released DOX from DOX&HAuNS-TSL was located in BEL-7402 cell nuclei.

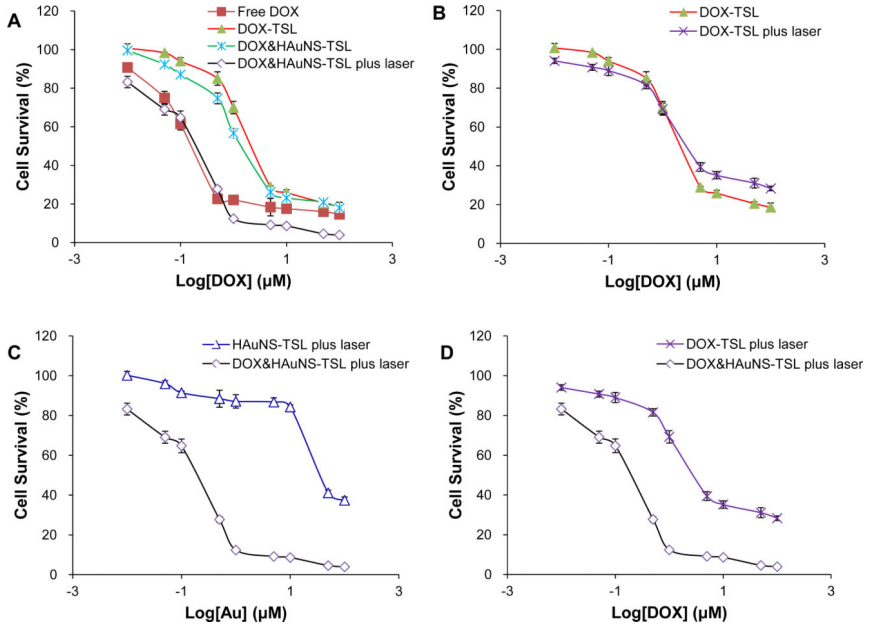

Figure 3.

(A) BEL-7402 cell viability as a function of HAuNS or DOX concentration. (A) Cells were treated with DOX&HAuNS-TSL plus NIR laser (diamond), DOX&HAuNS-TSL alone (cross), DOX-TSL alone (solid triangle) and free DOX (solid square). (B) Cells were treated with DOX-TSL with (square) or without (solid triangle) NIR laser irradiation. (C) Cells were treated with DOX&HAuNS-TSL plus NIR laser (diamond) or HAuNS-TSL plus NIR laser (triangle). (D) Cells were treated with DOX&HAuNS-TSL plus NIR laser (diamond) or DOX-TSL plus NIR laser (square).

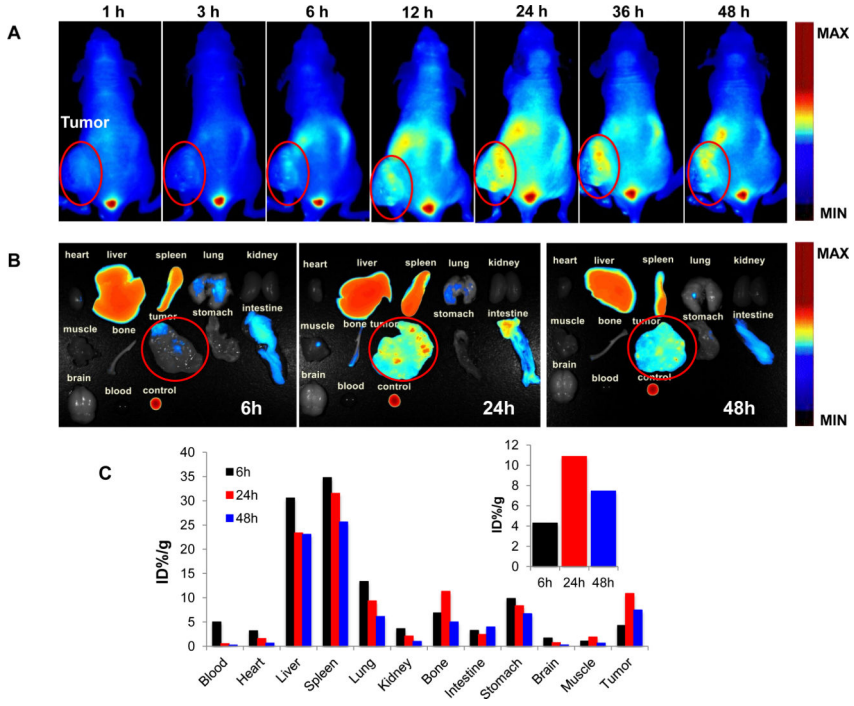

Figure 4.

(A) The in vivo imaging of the mice, bearing BEL-7402, at different time after iv injection of DiR marked DOX&HAuNS-TSL. (B) The fluorescent imaging of various tissues at 6, 24, and 48h after the iv injection of the liposomes. (C) The accumulation of DOX&HAuNS-TSL in various tissues was calculated as %ID/g (the percentage of the injected dose per gram of tissue). The fluorescent intensity, responding the amount of the liposomes, was read by the imaging system. Inset: The accumulation of DOX&HAuNS-TSL in tumors at 6, 24, and 48 h.

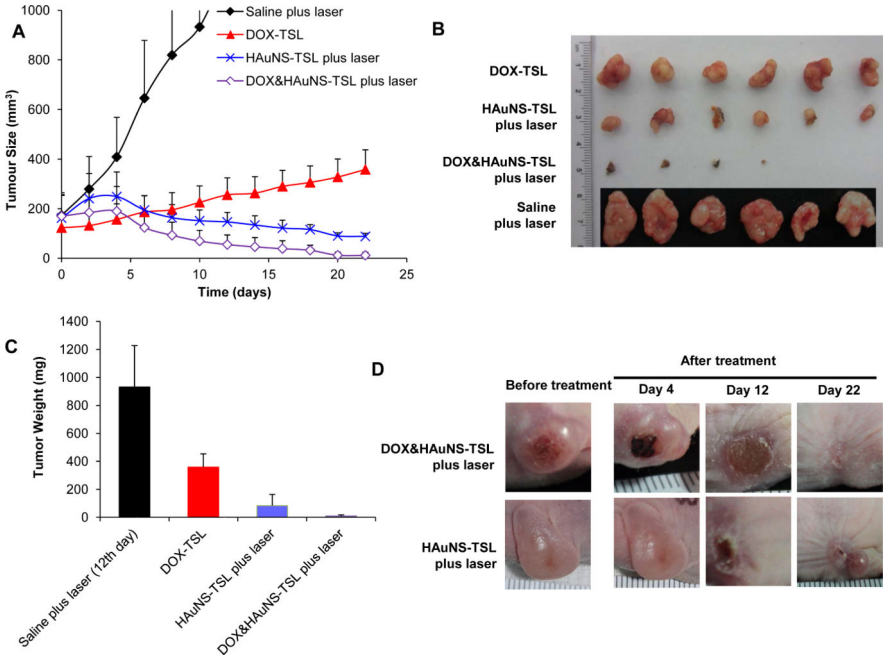

Figure 5.

Antitumor activity of various treatments against BEL-7402 tumors. (A) tumor growth curves for mice treated with saline plus NIR laser (n=6), HAuNS-TSL plus NIR laser (n=6), DOX-TSL alone (n=6), and DOX&HAuNS-TSL plus NIR laser (n=6). All mice were injected for total three times, and all tumors in mice, except the group of DOX-TSL, were irradiated by NIR laser (2.0 W/cm^2 for 5 minutes) for total three times at 24h after each injection. (B) Photographs of tumors and (C) average tumor weights in different treatment groups. Tumors were removed on day 22 for all groups except the saline plus laser group, in which tumors were removed on day 12. (D) Representative photographs of tumors in DOX&HAuNS-TSL plus NIR laser and HAuNS-TSL plus NIR laser before and after the treatment.

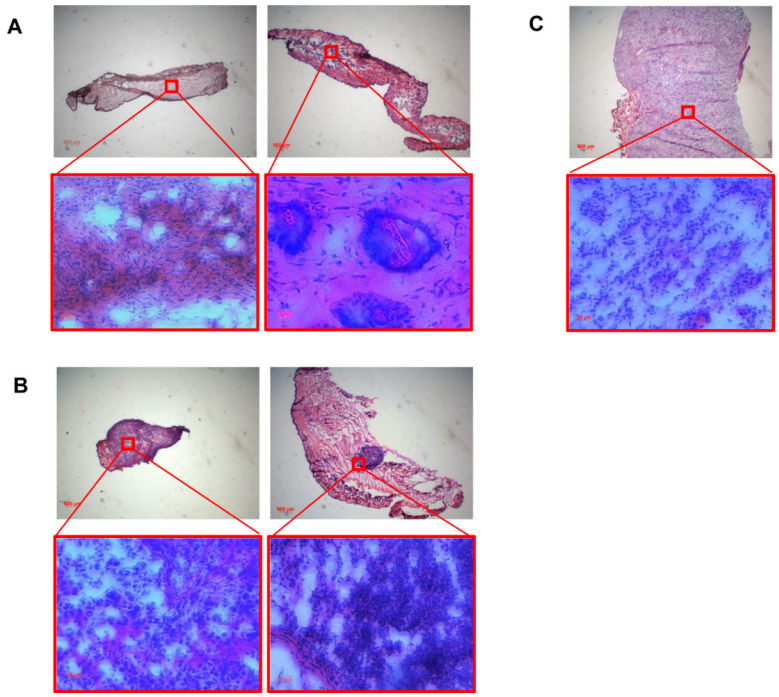

Figure 6.

Representative photomicrographs of hematoxylin and eosin (H&E)–stained slides from scar tissue (A, left) and residual tumor (A, right) from the mice treated with DOX&HAuNS-TSL plus NIR laser. Representative photomicrographs of H&E– stained slides from residual tumor (B, left) and scar tissue (B, right) from the mice treated with HAuNS-TSL plus NIR laser. (C) Representative photomicrographs of H&E–stained slides of the tumor in saline group.